

# Adiponectin improves diabetic nephropathy by inhibiting necrotic apoptosis

Wei Yi<sup>1</sup>, Qian OuYang<sup>2</sup>

<sup>1</sup>Department of Nephrology, The Fourth Affiliated Hospital of Nanchang University, Nanchang, Jiangxi, China

<sup>2</sup>Department of Critical Care Medicine, Jiangxi Provincial Tumor Hospital, Nanchang, Jiangxi, China

**Submitted:** 20 September 2018

**Accepted:** 17 October 2018

Arch Med Sci 2019; 15 (5): 1321–1328

DOI: <https://doi.org/10.5114/aoms.2018.79570>

Copyright © 2018 Termedia & Banach

**Corresponding author:**

Qian OuYang  
Department of  
Critical Care  
Medicine  
Jiangxi Provincial  
Tumor Hospital  
519 East Beijing Road  
Donghu District  
Nanchang City 330029  
Jiangxi Province, China  
Phone: +86 0791 88307527  
Fax: +86 0791-88307527  
E-mail: [qianouyang@outlook.com](mailto:qianouyang@outlook.com)

## Abstract

**Introduction:** This study aimed to investigate the effect of adiponectin (Apn) on necrotic apoptosis (Nec) *in vitro* and *in vivo* to clarify the possible role of Apn in the pathogenesis of diabetic nephropathy (DN).

**Material and methods:** Rat glomerular endothelial (RGE) cells were treated with high glucose (HG, 30 mmol/l) for 24 h and the effects of Apn on cell viability, RIP1 and RIP3 expression and p-p38MAPK activation were assayed by CCK-8, immunofluorescence and western blot. Then a streptozotocin (STZ)-induced DN rat model was established. The body weight, left kidney weight, left kidney weight/body weight (KW/BW), creatinine clearance rate (Ccr), 24 h urine protein and blood glucose were recorded. The expression of RIP1, RIP3 and p-p38MAPK in renal tissues was examined by immunohistochemistry and western blot.

**Results:** Treatment of RGE cells with HG induced significant cytotoxicity and increased expression levels of RIP1, RIP3 and p-p38MAPK, which were abrogated by Apn in a concentration-dependent manner. *In vivo*, compared with the control group, the Ccr, 24 h urine protein and the blood glucose level of the rats in the model group were significantly increased, effects which were abrogated by Apn intervention. Moreover, the expression levels of RIP1, PIP3 and p-p38MAPK were also significantly increased in the model group, effects which were canceled by Apn intervention.

**Conclusions:** Apn can alleviate the inflammatory response and damage of DN by inhibiting Nec via p-p38MAPK signaling.

**Key words:** rat glomerular endothelial cells, diabetic nephropathy, necroptosis, p38MAPK.

## Introduction

Diabetic nephropathy (DN) is one of the common and serious micro-vascular complications of diabetes mellitus (DM). It is clinically characterized by proteinuria, edema and hypertension, and it further develops into azotemia and renal failure. 30–40% of the patients with a 15-year course of diabetes have DN, which is the leading cause of death in diabetic patients. The occurrence and development of DN is related to a variety of factors, including genetic susceptibility, glomerular sclerosis and hemodynamic changes, urinary albumin excretion, glucose toxicity [1–3] and so on.

Adiponectin (Apn) was first isolated and cloned in the mouse 3T3-L1 adipocyte cell line in 1995. It is named as adipocyte complement-associated protein 30 and is a specific protein secreted by adipocytes with a molecular mass of about 30 kD [4]. In recent years, studies have found that Apn has a certain correlation [5, 6] with obesity, type 2 DM, insulin resistance, atherosclerosis and diabetic vascular disease. It has been confirmed by animal experiments that insulin resistance is improved and blood glucose levels are reduced after injection of recombinant Apn into obese mice, suggesting that Apn has an important protective effect on diabetic damage [7].

In 2005, Degterev *et al.* reported a new way of cell death: Necroptosis (Nec) [8] is programmed cell death, which has morphological features similar to necrosis, while the cell death pattern is non-caspase-dependent, that is, the combination of death receptor and ligand can trigger necrotic apoptosis under the condition of caspase inhibition. Tumor necrosis factor (TNF)  $\alpha$  combining with TNFR1 on the plasma membrane causes the TNF receptor associated death domain (TRADD) to send receptor interacting protein 1 (RIP1) signals to recruit RIP3, thereby forming a necrosome [9].

Inflammation is the main cause of Nec and increases the incidence rate of cardiovascular events in diabetic patients and the death rate of patients with renal failure [10]. Signal transduction pathways of mitogen-activated protein kinases (MAPKs) are the most critical pathways in the inflammatory transduction network [11]. This study aimed to investigate the effect of Apn on necrotic apoptosis of rat glomerular endothelial cells under high glucose (HG) and renal tissue in diabetic animal models, to clarify the possible role of Apn in the pathogenesis of DN and its signaling, and to provide a new theoretical basis for the prevention and treatment of DN.

## Material and methods

### Cell culture

Rat glomerular endothelial (RGE) cells were purchased from ATCC, USA, incubated in DMEM medium containing 10% fetal bovine serum (FBS) and maintained in 5% CO<sub>2</sub> at 37°C. When the cell density reached 90%, the cells were digested and counted; 10<sup>5</sup> cells were inoculated into new culture flasks, cultured to 80% fusion in DMEM medium containing 15% FBS, and then synchronously cultured in serum-free medium for 24 h. Subsequently, they were divided into a control group (5 mmol/l glucose), HG group (30 mmol/l glucose), ApnL group (30 mmol/l glucose + 1  $\mu$ g/ml Apn), ApnM group (30 mmol/l glucose + 5  $\mu$ g/ml Apn),

ApnH group (30 mmol/l glucose + 25  $\mu$ g/ml Apn), and mannitol group (5 mmol/l glucose + 25 mmol/l mannitol), and continued to culture for 24 h.

### Cell viability [12] was determined by CCK-8

RGE cells were inoculated in a 96-well culture plate. When the cells were grown to about 80% fusion, the above grouping was performed. They were incubated for different periods, then the supernatant was discarded, and washed 3 times with PBS; 90  $\mu$ l of DMEM and 10  $\mu$ l of CCK-8 were added to each well, incubated for 2.5 h in a 37°C incubator, and absorbance density (OD 490 nm) of the wells was recorded with a microplate reader. This experiment was repeated 5 times.

### Animal model establishment

This study was approved by the Ethics Committee of Nanchang University and conducted in accordance with the Declaration of Helsinki and the Guide for the Care and Use of Laboratory Animals. Thirty male, standard, clean, healthy Sprague-Dawley (SD) rats were provided by the Experimental Animal Center.

Diabetes model preparation: STZ was dissolved in citrate buffer (pH = 4.5) in the weight ratio of 60 mg/kg; under fasting conditions, intraperitoneal injection was performed; the normal control group was only injected with an equal amount of citrate buffer. The blood glucose level was measured at 72 h, and  $\geq 16.7$  mmol/l indicated that the diabetes animal model was successfully established. Among the 30 rats, in 28 the blood sugar reached the standard, with a success rate of 93.3%.

DN model preparation: 24 h urine protein was measured at 4 weeks, and  $\geq 30$  mg/day indicated that the DN models were successfully established. Among the 28 rats, 20 reached the standard, with a success rate of 71.4%. The successful DN animal model was randomly divided into a model group ( $n = 10$ ) and a DN/Apn group ( $n = 10$ ), and 2 mg/kg/day Apn was injected into the tail vein of the rat models in the DN/Apn group for 6 weeks. Eight SD rats with matched age and body weight were finally selected as the normal control group. At the end of the study, the animals were injected with isoflurane overdose and subjected to cervical dislocation to sacrifice the animals.

### Collection and testing of specimens

In 6 weeks after the Apn administration, the rats were placed in a metabolic cage, and urine was collected in 24 h. After filtration, the rats' urine was stored at -70°C for urine protein quantification. Serum creatinine and urine creatinine were measured using an automatic biochemical analyzer, and the creatinine clearance rate (Ccr)

was calculated using the following equation:  $Ccr = \text{urine creatinine} \times \text{urine volume} / \text{serum creatinine} \times 1440 / \text{body weight}$ . Then, the rats were weighed, anesthetized by intraperitoneal injection with sodium pentobarbital at a weight ratio of 45 mg/kg, and the left kidneys of the rats were quickly weighed. After the right kidney was lavaged with normal saline, some right kidney tissues were taken and fixed with 10% neutral formaldehyde, and embedded in paraffin for immunohistochemistry and hematoxylin-eosin (HE) staining. Some kidney tissues were taken separately for western blot analysis.

### Renal pathologic examination

Renal tissue was fixed with 10% neutral formaldehyde, embedded in paraffin, sliced in sections 4  $\mu\text{m}$  thick, and stained with HE in order to observe the degree of mesangial matrix hyperplasia as well as glomerular, renal tubule and renal interstitial lesions. Glomerular hypertrophy was confirmed by measuring the mean glomerular diameter of 20 glomeruli. Renal tissue sections were routinely dewaxed and dehydrated, incubated in 3% hydrogen peroxide for 10 min at room temperature to eliminate endogenous peroxidase, and blocked with serum for 10 min, then rabbit anti-rat RIP1 and PIP3 antibody were added (1 : 200, overnight at 4°C), and washed with phosphate buffer saline (PBS) twice, 3 min each time. On the next day, biotin-labeled secondary antibody was added to each section, incubated at 37°C for 30 min, and then washed twice with PBS, 3 min each time. Next, HRP-labeled streptavidin was added to each section, incubated at 37°C for 30 min, and then washed twice with PBS, 3 min each time. After they were developed with diaminobenzidine (DAB) for 5–20 min at room temperature, they were slightly counterstained with hematoxylin-eosin.

### Western blotting

Cells or kidney tissues were lysed on ice for 30 min with cell lysis solution (containing protease inhibitor cocktail). They were centrifuged at 12 000  $\times$  g for 15 min at 4°C, and then the supernatant was taken. Protein quantification was performed by the bicinchoninic acid (BCA) method. A 50  $\mu\text{g}$  sample was loaded in each group, and subjected to sodium dodecyl sulfate polyacrylamide gel electrophoresis (SDS-PAGE) using 5% concentrated gel and 8% or 10% separating gel to separate the proteins (RIP1, PIP3, p-p38MAPK and t-p38MAPK). These proteins were transferred to a polyvinylidene fluoride (PVDF) membrane at 220 mA electric current for 1 h; then they were blocked for 1 h at room temperature; after that

they were washed 3 times with tris buffered saline Tween (TBST), and the corresponding primary antibodies were incubated overnight at 4°C. The next day, they were incubated with corresponding secondary antibody for 1 h at room temperature; then, they were incubated with an enhanced chemiluminescence solution for 2 min, and quantified using Alpha-Ease software version 2200 [13].

### Statistical analysis

Statistical analysis was performed using SPSS 19 statistical software. The measurement data were expressed by mean  $\pm$  SD, and the comparison between groups was made by analysis of variance (ANOVA).  $P < 0.05$  indicated that the difference was statistically significant.

## Results

### Apn protected HG-induced Nec

Figure 1 A shows that treatment of RGE cells with HG (30 mmol/l) for 24 h can induce significant cytotoxicity and thus reduce cell viability; compared with the normal control group, the difference is statistically significant. The cell viability was increased by co-treatment of the cells with 1, 5 or 25  $\mu\text{g}/\text{ml}$  Apn and HG for 24 h, which was statistically significant ( $p < 0.05$ ); the inhibitory effect of 25  $\mu\text{g}/\text{ml}$  Apn on cytotoxicity was most pronounced.

We tested the expression of RIP1 and RIP3 in cells by further application of immunofluorescence and western blot. The expression levels of RIP1 and RIP3 in cells treated with HG for 24 h were significantly increased. Co-treatment of cells with 1, 5 or 25  $\mu\text{g}/\text{ml}$  Apn and HG for 24 h could reduce the expression of RIP1 and RIP3. The differences were statistically significant (Figures 1 B, C).

The expression of p-p38MAPK was also significantly increased by treating the cells with HG for 24 h; compared with the normal control group, the difference was statistically significant ( $p < 0.01$ ). The expression of p-p38MAPK was significantly decreased by co-treatment of cells with 1, 5 or 25  $\mu\text{g}/\text{ml}$  Apn and HG for 24 h ( $p < 0.01$ , Figure 1 C).

### Apn improved DN

After 10 weeks, STZ rats clearly showed symptoms of polydipsia, polyuria and polyphagia, and their body weights were significantly reduced. In addition to the death of 3 rats in the model group, the animals in other groups were in a good condition. The body weight, left kidney weight, left kidney weight/body weight (KW/BW, g/kg), Ccr, urine protein and blood glucose for each group of rats are shown in Figure 2. Compared with the rats in the control group, the body weights of the

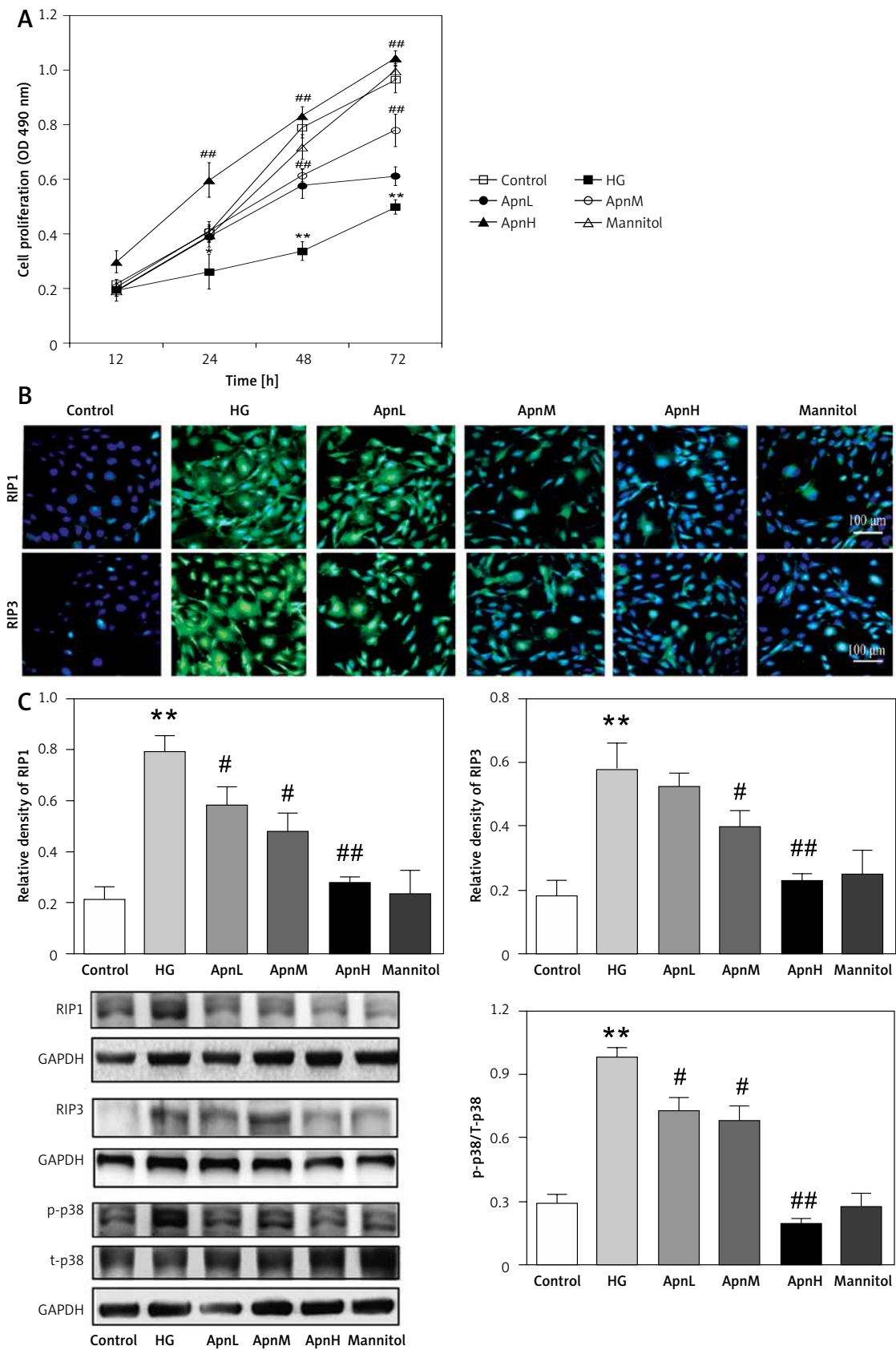


**Figure 1.** Apn protects HG-induced Nec. **A** – Cell viability was assayed by CCK-8 assay. Treatment of RGE cells with HG (30 mmol/l) for 24 h can cause significant cytotoxicity. Cell viability was promoted by co-treatment of the cells with 1, 5 or 25  $\mu$ g/ml Apn. **B** – The expression of RIP1 and RIP3 in cells were examined by immunofluorescence. **C** – The expression of RIP1, RIP3 and p-p38MAPK were assayed by western blot. The expression levels of RIP1, RIP3 and p-p38MAPK in HG-treated cells were significantly increased. Co-treatment of cells with 1, 5 or 25  $\mu$ g/ml Apn could reduce the expression of RIP1, RIP3 and p-p38MAPK

\* $p < 0.05$  and \*\* $p < 0.01$  vs. Control; # $p < 0.05$  and ## $p < 0.01$  vs. HG.

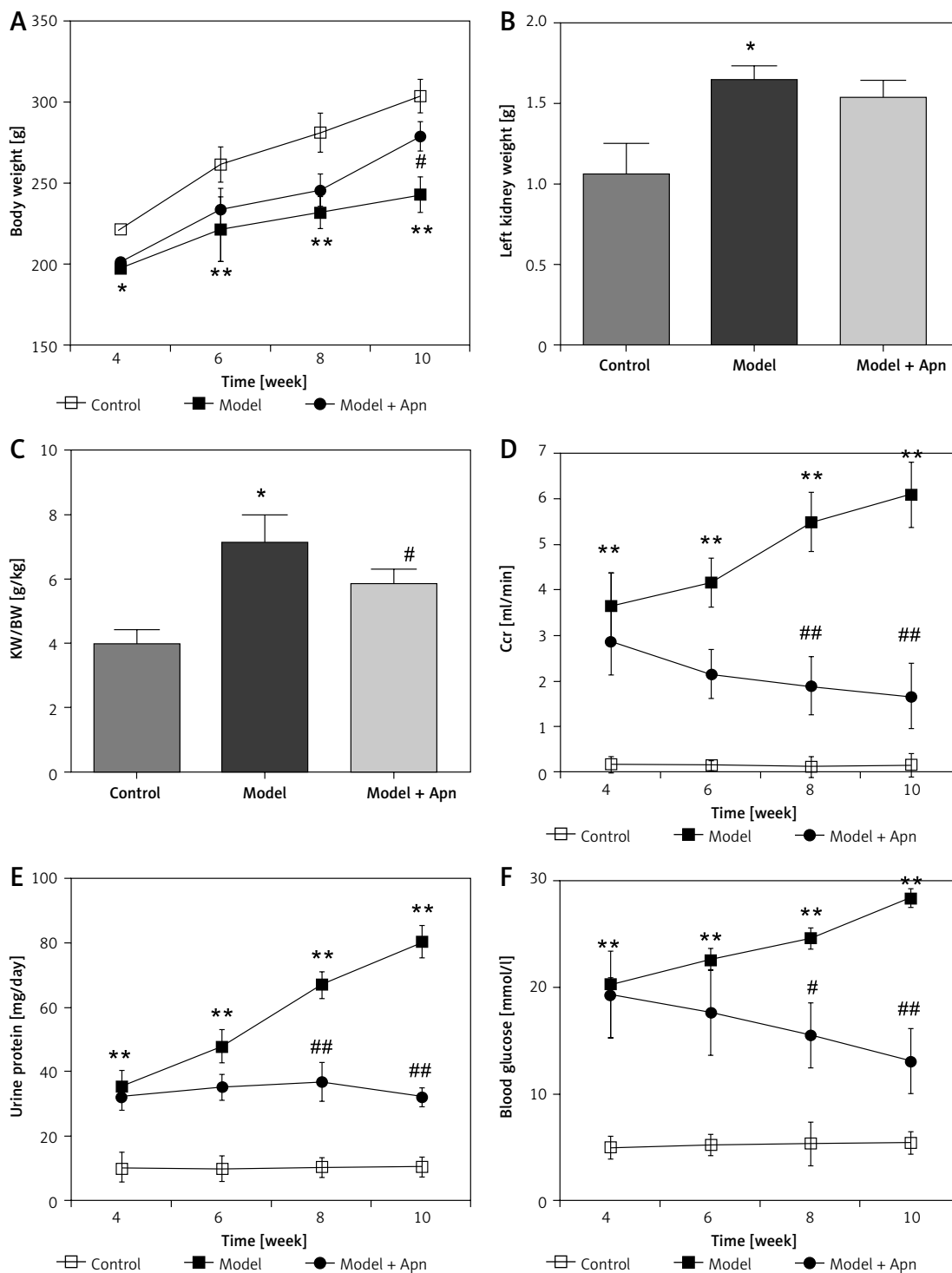


**Figure 2.** Apn improves DN animal models ( $n = 8$ ). Compared with the rats in the control group, the body weights of the rats in the model group were significantly reduced from the 4<sup>th</sup> week, and were increased from the 6<sup>th</sup> week after Apn intervention. The left kidney weight and KW/BW of the rats in the model group were significantly increased and KW/BW significantly decreased after Apn intervention. Ccr, 24 h urine protein and blood glucose from the rats in the model group increased significantly from the 4<sup>th</sup> week, and significantly decreased from the 4<sup>th</sup> week after Apn intervention

\* $p < 0.05$  and \*\* $p < 0.01$  vs. Control; # $p < 0.05$  and ## $p < 0.01$  vs. Model.

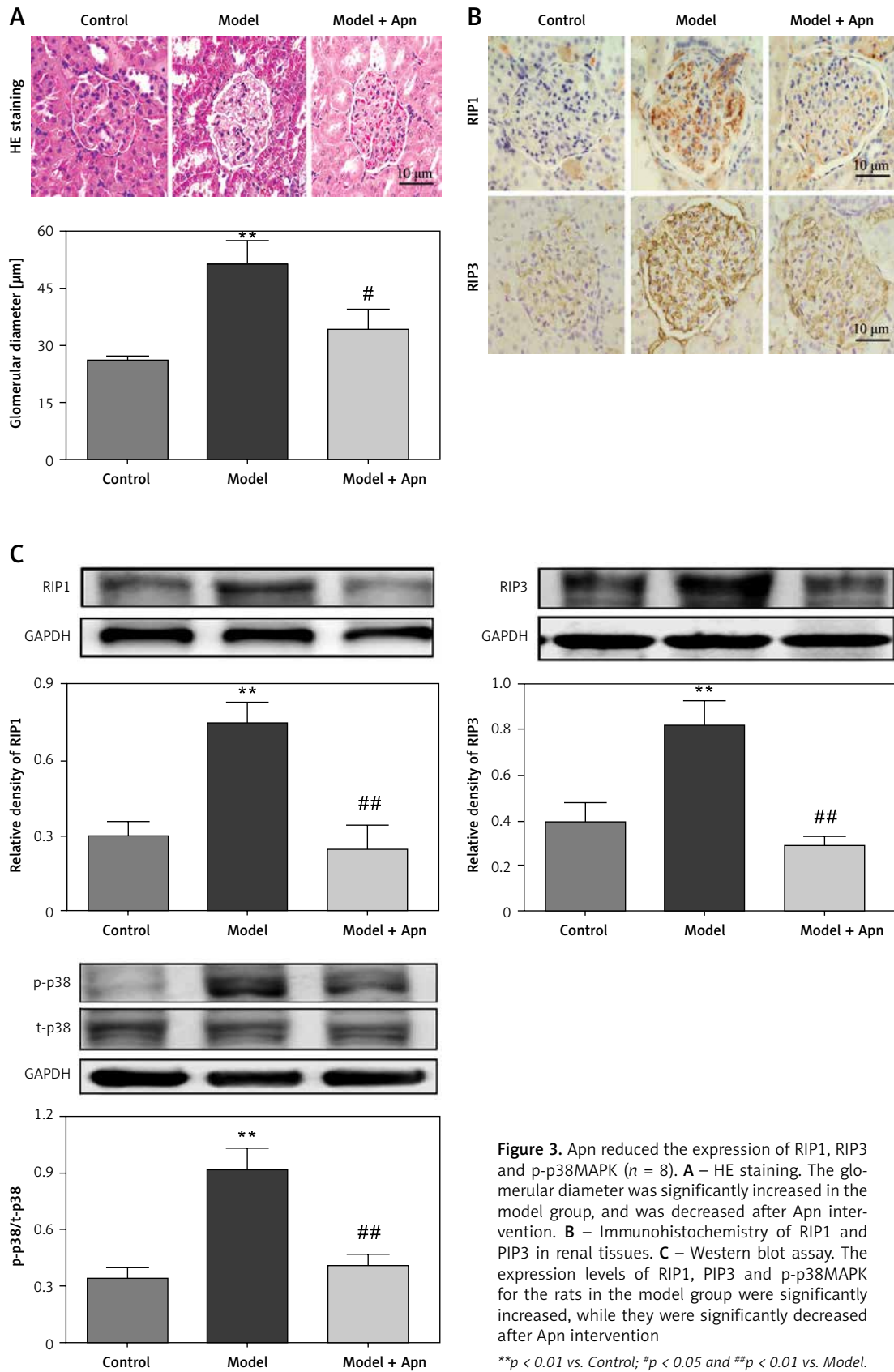


**Figure 3.** Apn reduced the expression of RIP1, RIP3 and p-p38MAPK ( $n = 8$ ). **A** – HE staining. The glomerular diameter was significantly increased in the model group, and was decreased after Apn intervention. **B** – Immunohistochemistry of RIP1 and RIP3 in renal tissues. **C** – Western blot assay. The expression levels of RIP1, RIP3 and p-p38MAPK for the rats in the model group were significantly increased, while they were significantly decreased after Apn intervention

\*\* $p < 0.01$  vs. Control; # $p < 0.05$  and ## $p < 0.01$  vs. Model.

rats in the model group were significantly reduced from the 4<sup>th</sup> week; the body weights of the rats increased from the 6<sup>th</sup> week after Apn intervention ( $p < 0.05$ ). KW/BW (g/kg) of the rats in the model group was significantly increased, and decreased after Apn intervention. Ccr, 24 h urine protein and blood glucose levels of the rats in the model group increased significantly from the 4<sup>th</sup> week ( $p < 0.01$ ), while they significantly decreased from the 4<sup>th</sup> week after Apn intervention ( $p < 0.01$ ).

#### Apn reduced the expression of RIP1, RIP3 and p-p38MAPK

HE staining showed that, for the rats with DN, their glomerular diameters were significantly increased (greater than the rats in the control group), their glomerular mesangial matrix was proliferated, focal lymphocytes and monocyte infiltration were observed in the interstitial region, and some of the epithelial cells of the renal tubules began to develop vacuolar degeneration and even partially fall off. Compared with the rats in the model group, the glomerular capillary loops of the rats in the Apn group were well opened, the mesangial matrix was slightly proliferated, a small amount of inflammatory cells infiltrated, and some renal tubular epithelial cells began to repair (Figure 3 A). The results of immunohistochemistry of RIP1 and PIP3 in renal tissues showed that RIP1 and PIP3 were mainly expressed in renal tubules of the kidney tissues of DN rats (Figure 3 B). Western blot results showed that the expression levels of RIP1 and PIP3 proteins of the rats in the model group were significantly increased, and were significantly decreased after Apn intervention (Figure 3 C). Moreover, the activation of p-p38MAPK in renal tissue of DN rats was also significantly increased, and was significantly decreased after Apn intervention (Figure 3 C).

#### Discussion

DN is one of the common chronic complications of diabetes, and Nec plays an important role in its pathogenesis [14]. It has been confirmed that it involves the participation of RIP1 and RIP3. RIP1 is the first confirmed important molecule that regulates programmed cell necrosis under the conditions in which caspase is inhibited. RIP1, as an upstream kinase, can regulate RIP3-dependent programmed necrosis, and induce formation [15] of the RIP1-RIP3 necrosome under the action of TNF- $\alpha$ .

According to modern endocrinology, adipose tissue is not only the main energy storage organ, but also an endocrine organ of the body, and meanwhile it can also secrete a variety of biologically active factors. Previous studies found that Apn has the functions of improving insulin sensitivity,

lowering blood glucose and blood lipid, resisting atherosclerosis, inhibiting inflammatory reactions, resisting immunity and protecting microvessels [16, 17]. The results of this experiment showed that the expression of RIP1 and RIP3 in RGE cells was significantly decreased under HG stimulation after Apn intervention in a concentration-dependent manner, indicating that Apn might reduce the inflammatory response and damage of RGE cells and promote cell repair by inhibiting the Nec pathway. The p38MAPK pathway is one of the important members of the MAPK family, can be activated by various stimuli such as inflammation, ischemia, hypoxia, chemical damage, etc., and can participate in the regulation of pathological and physiological processes [18] such as cell growth, differentiation and apoptosis. Our study suggests that the p38MAPK pathway can mediate HG-induced cell damage. Apn can significantly inhibit the up-regulation of p-p38MAPK expression caused by HG, suggesting that Apn can inhibit Nec and improve DN by inhibiting the p38MAPK signaling pathway.

STZ specifically destroys islet  $\beta$ -cells and different doses of STZ induce different degrees of islet damage. A large dose of STZ (60 mg/kg) induces diabetes similar to the acute phase of human type I diabetes [19]. In the present study, we found that proteinuria in rats increased significantly at 4 weeks, and increases progressively with time. In animal models, we found that Apn significantly improved DN including increasing the body weight and KW/BW and decreasing Ccr, 24 h urine protein and blood glucose. Also, Apn reduced the expression of RIP1, RIP3 and p-p38MAPK and decreased the expression of RIP1 and RIP3.

In conclusion, Apn can alleviate the inflammatory response and damage of DN by inhibiting the Nec pathway via the p38MAPK pathway.

#### Conflict of interest

The authors declare no conflict of interest.

#### References

- Gantala SR, Kondapalli MS, Kummari R, et al. Collagenase-1 (-1607 1G/2G), gelatinase-A (-1306 C/T), stromelysin-1 (-1171 5A/6A) functional promoter polymorphisms in risk prediction of type 2 diabetic nephropathy. *Gene* 2018; 673: 22-31.
- Zoja C, Locatelli M, Corna D, et al. Therapy with a selective cannabinoid receptor type 2 agonist limits albuminuria and renal injury in mice with type 2 diabetic nephropathy. *Nephron* 2016; 132: 59-69.
- Kaifu K, Ueda S, Nakamura N, et al. Advanced glycation end products evoke inflammatory reactions in proximal tubular cells via autocrine production of dipeptidyl peptidase-4. *Microvasc Res* 2018; 120: 90-3.
- Scherer PE, Williams S, Fogliano M, Baldini G, Lodish HF. A novel serum protein similar to C1q, produced exclusively in adipocytes. *J Biol Chem* 1995; 270: 26746-9.

5. Abdella NA, Mojiminiyi OA. Clinical applications of adiponectin measurements in type 2 diabetes mellitus: screening, diagnosis, and marker of diabetes control. *Dis Markers* 2018; 2018: 5187940.
6. Zhang CJ, Deng YZ, Lei YH, Zhao JB, Wei W, Li YH. The mechanism of exogenous adiponectin in the prevention of no-reflow phenomenon in type 2 diabetic patients with acute myocardial infarction during PCI treatment. *Eur Rev Med Pharmacol Sci* 2018; 22: 2169-74.
7. Hu X, She M, Hou H, et al. Adiponectin decreases plasma glucose and improves insulin sensitivity in diabetic Swine. *Acta Biochim Biophys Sin (Shanghai)* 2007; 39: 131-6.
8. Degtarev A, Huang Z, Boyce M, et al. Chemical inhibitor of nonapoptotic cell death with therapeutic potential for ischemic brain injury. *Nat Chem Biol* 2005; 1: 112-9.
9. Tran AHV, Han SH, Kim J, Grasso F, Kim IS, Han YS. MutY DNA glycosylase protects cells from tumor necrosis factor alpha-induced necroptosis. *J Cell Biochem* 2017; 118: 1827-38.
10. Gupta K, Phan N, Wang Q, Liu B. Necroptosis in cardiovascular disease – a new therapeutic target. *J Mol Cell Cardiol* 2018; 118: 26-35.
11. Obeid S, Wankell M, Charrez B, et al. Adiponectin confers protection from acute colitis and restricts a B cell immune response. *J Biol Chem* 2017; 292: 6569-82.
12. Li L, Liu M, Kang L, et al. HHEX: a crosstalk between HCMV infection and proliferation of VSMCs. *Front Cell Infect Microbiol* 2016; 6: 169.
13. Wang L, Wu G, Qin X, et al. Expression of nodal on bronchial epithelial cells influenced by lung microbes through DNA methylation modulates the differentiation of T-helper cells. *Cell Physiol Biochem* 2015; 37: 2012-22.
14. Meng XM, Ren GL, Gao L, et al. NADPH oxidase 4 promotes cisplatin-induced acute kidney injury via ROS-mediated programmed cell death and inflammation. *Lab Invest* 2018; 98: 63-78.
15. Zhang Y, Su SS, Zhao S, et al. RIP1 autophosphorylation is promoted by mitochondrial ROS and is essential for RIP3 recruitment into necrosome. *Nat Commun* 2017; 8: 14329.
16. Lin Z, Pan X, Wu F, et al. Fibroblast growth factor 21 prevents atherosclerosis by suppression of hepatic sterol regulatory element-binding protein-2 and induction of adiponectin in mice. *Circulation* 2015; 131: 1861-71.
17. Kim K, Li J, Tseng A, Andrews RK, Cho J. NOX2 is critical for heterotypic neutrophil-platelet interactions during vascular inflammation. *Blood* 2015; 126: 1952-64.
18. Yang L, Xu F, Zhang M, et al. Role of LncRNA MALAT-1 in hypoxia-induced PC12 cell injury via regulating p38MAPK signaling pathway. *Neurosci Lett* 2018; 670: 41-7.
19. Vinerean HV, Gazda LS, Hall RD, Smith BH. Streptozotocin is responsible for the induction and progression of renal tumorigenesis in diabetic Wistar-Furth rats treated with insulin or transplanted with agarose encapsulated porcine islets. *Islets* 2011; 3: 196-203.